Geochemical Perspectives Letters

Earth's deep magma ocean never reached sulfide saturation

I. Blanchard[1*], J. Siebert[2], E. Kubik[3], A. Minchenkova[3], L. Calvo[2], N. Wehr[2]

https://doi.org/10.7185/geochemlet.2506

Abstract

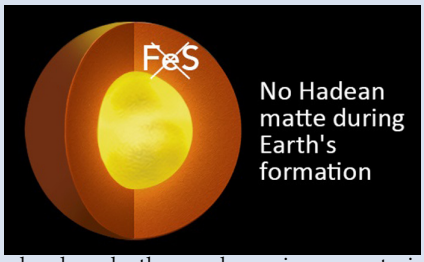

The chondritic abundances of highly siderophile elements in the Earth's mantle have been proposed to result from the combination of pervasive exsolution and segregation of sulfide from the magma ocean, along with late accretion. Therefore, evaluating the sulfur storage capacity (*i.e.* sulfur solubility) of the deep magma ocean is key to understanding the late stages of Earth's formation. Here, we have investigated the effects of high pressure and high temperature on the solubility of sulfur in the deep primordial magma ocean by melting and equilibrating a pyrolytic glass with pure FeS in a laser-heated diamond anvil cell. Chemical analysis of the run products show that significant amounts of sulfur can be stored deep in the magma ocean (~1 wt. %). We developed a thermodynamic parameterisation predicting the solubility of sulfur at sulfide saturation (SCSS) depending on pressure, temperature and silicate composition. We show that SCSS always exceeds the amount of sulfur present in the mantle due to metal-silicate partitioning, consistent with previous work. Consequently, it appears that Earth's magma ocean likely never reached sulfur saturation, thereby preventing the segregation of a sulfide-rich melt, also referred as the "Hadean matte".

Received 27 September 2024 | Accepted 17 January 2025 | Published 20 February 2025

Introduction

The formation of Earth's main reservoirs, the metallic core and the surrounding silicate mantle, occurred early in Earth's history. During the first few tens of million years, the Earth was covered by a deep magma ocean with pressure and temperature conditions exceeding 40 GPa and 3000 K respectively (Li and Agee, 1996; Siebert *et al.*, 2012). These conditions led to the separation of siderophile (iron-loving) from lithophile elements (silicate-loving) to form the core and the mantle, respectively. Understanding how the Bulk Silicate Earth (BSE) composition was established is of primary importance, and is directly linked to our comprehension of the Earth's differentiation as well as the accretion process and the nature of Earth's building blocks.

Sulfur is a key element for understanding Earth's formation. It has been proposed that the mantle's signature in Highly Siderophile Elements (HSEs) could be explained by HSE segregation into a sulfide matte exsolved from the magma ocean towards the end of accretion (O'Neill, 1991; Rubie *et al.*, 2016). For this hypothesis to hold, the magma ocean must have reached sulfur saturation, enabling the segregation of a sulfide matte. The solubility of sulfur at sulfide saturation (SCSS) in molten silicate has been the subject of numerous studies, focusing mainly on the effects of the silicate composition on SCSS (Liu *et al.*, 2007; Fortin *et al.*, 2015; Namur *et al.*, 2016). Recently, the effects of pressure (P) and temperature (T) have been studied (Laurenz *et al.*, 2016; Blanchard *et al.*, 2021; Steenstra *et al.*, 2022), but either at limited P–T conditions (Laurenz *et al.*, 2016; Blanchard *et al.*, 2021) or using basalt as starting composition, which might not be relevant in the context of the Earth's formation (Steenstra *et al.*, 2022).

In this work, we have used a laser-heated diamond anvil cell (LH-DAC) to replicate the high P–T conditions of Earth's differentiation in the laboratory. We have equilibrated a pyrolytic melt with pure FeS and showed that sulfur solubility in silicate melt remains high under these conditions. Additionally, we have also used a basaltic composition to compare our results with those reported by Steenstra *et al.*, (2022). Our experimental results, along with data from the literature, were used to parameterise a model predicting the evolution of sulfur saturation in a deep magma ocean. We show that SCSS remains significantly high throughout the accretion process, with mean values around 3000 ppm.

In contrast, sulfur content in the mantle produced from metal-silicate partitioning is always much lower (<600 ppm; Suer *et al.*, 2017). Hence, it seems unlikely that sulfur saturation was achieved during Earth's differentiation. This challenges the Hadean Matte hypothesis and suggests that alternative mechanisms should be considered to explain the budget of HSEs of the mantle.

Methods

We synthetised five samples between 53 and 72 GPa and 3800 to 4050 K using a laser-heated diamond anvil cell. Synthetic pyrolytic and basaltic glasses were melted and equilibrated with pure FeS. Experimental runs were subsequently recovered using Focused Ion Beam (FIB) and analysed using scanning electron

1. Institut de Minéralogie de Physique de la Matière et de Cosmochimie, Sorbonne Université, CNRS, Paris, France
2. Université Paris Cité, Institut de Physique du Globe de Paris, CNRS, Paris, France
3. Bayerisches Geoinstitut, Universität Bayreuth, Bayreuth, Germany
* Corresponding author (email: ingrid.blanchard@sorbonne-universite.fr)

Table 1 Summary of experimental conditions.

Starting Material	Experiment	P (GPa)	T (K)	ΔIW	SCSS (wt. %)
Pyrolite + FeS	SCSS1	64 ± 5	4000 ± 300	−1.31	1.02 ± 0.27
Pyrolite + FeS	SCSS2	61 ± 5	4000 ± 300	−1.27	1.12 ± 0.36
Pyrolite + FeS	SCSS3	72 ± 5	4050 ± 300	−1.64	1.15 ± 0.15
Basalt + FeS	SCSS4	53 ± 5	3800 ± 300	−0.92	0.83 ± 0.31
Pyrolite + FeS	SCSS5	53 ± 5	3800 ± 300	−1.42	0.93 ± 0.25

microscopy energy dispersive X-rays. More details of the experimental and analytical procedures are given in the Supplementary Information. Table 1 summarises experimental conditions while Table S-1 gives the full chemical analysis of each run.

Experimental Results

Each run consisted of a spherical sulfide blob surrounded by a quench silicate melt (see Figs. 1, S-1). The silicate melt of experiments performed using pyrolite as starting glass (SCSS1, 2, 3 and 5) or basaltic glass (SCSS4) fall in the range of terrestrial peridotites or basalts respectively. The amount of sulfur in the silicate melt from SCSS4 is slightly lower than in the other experiments, although the experimental runs look similar (see Fig. 1). The sulfide phase contains between 25 and 29 wt. % sulfur, along with roughly 6 to 10 wt. % oxygen, and 0.58 to 1.17 wt. % Si. This oxygen concentration is similar to that observed in previous metal-silicate partitioning diamond anvil cell experiments containing no sulfur. The concentration of silicon in sulfide is similar to observations from Steenstra *et al.* (2022), but much lower than in experiments containing no sulfide (*e.g.*, Blanchard *et al.*, 2017; Fischer *et al.*, 2020; Huang *et al.*, 2021). Traces of Mg and Al were also detected in the sulfide (see Table S-1). Overall, the compositions of the sulfide phases are similar, regardless of whether the starting material was pyrolytic or basaltic glass. We calculated the redox conditions of our experiments relative to the iron-wüstite buffer (IW; see Supplementary Information), and derived values between −0.9 to −1.41, consistent with previous diamond anvil cell experiments on other systems (*e.g.*, Siebert *et al.*, 2012; Blanchard *et al.*, 2022). No chemical or textural differences were observed between samples for which the temperature was maintained for either 10 or 120 seconds, suggesting that equilibrium is likely achieved in a very short time.

Thermodynamics

The solubility of sulfur in a magma ocean is intrinsically linked to the evolution of SCSS with pressure and temperature. To date, no study has focused on the effects of P and T in a system relevant for Earth's formation, specifically a pyrolytic magma ocean. Apart from the effects of pressure and temperature, it is well documented that the composition of the silicate itself has an impact on SCSS (Liu *et al.*, 2007; Fortin *et al.*, 2015; Namur *et al.*, 2016). Among the most important elements influencing SCSS, experimental works have shown that iron (FeO) and silicon (SiO_2) play major roles (O'Neill and Mavrogenes, 2002; Wykes *et al.*, 2015; Smythe *et al.*, 2017; Blanchard *et al.*, 2021). Recent use of machine learning has confirmed that Si and Fe in silicate are indeed among the most important parameters influencing SCSS (ZhangZhou *et al.*, 2024). While other components might also play a role, we chose not to overload our regression with parameters that are potentially not well constrained. Hence, we modelled SCSS following:

$$\ln S_{SCSS} = a + \frac{b}{T} + c\frac{P}{T} + \frac{d}{T} \times X_{FeO} + \frac{e}{T} \times X_{SiO_2} \qquad \text{Eq. 1}$$

with X_{FeO} and X_{SiO_2} as the mole fraction of FeO and SiO_2 respectively. We combined more than 200 data from the literature that cover a wide range of pressure (1 bar to 72 GPa), temperature (1573 to 4300 K) and silicate composition. Details of the selection is given in the Supplementary Information, and the final data set used for our parameterisation is provided in the Supplementary Information.

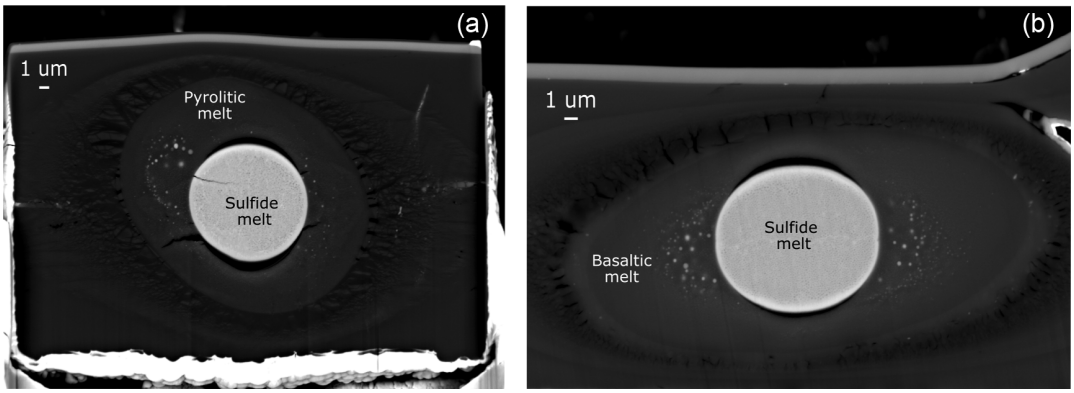

Figure 1 Backscattered images of two typical recovered runs. **(a)** Sample SCSS5 synthesised using pyrolytic glass as starting material, whereas **(b)** was synthetised with basaltic glass (SCSS4). Both runs were equilibrated at 53 GPa and 3800 K.

We obtain the following equation, with uncertainties in brackets:

$$\ln S_{SCSS} = 11.3\,(0.2) - \frac{4562\,(599)}{T} - 70(12)\frac{P}{T} + \frac{9740\,(783)}{T} \times X_{FeO} - \frac{5211\,(570)}{T} \times X_{SiO_2} \quad \text{Eq. 2}$$

Equation 2 shows that SCSS decreases with increasing pressure and X_{SiO_2}, and increases with increasing T and X_{FeO}. The effects of pressure and temperature that we derive from this study are coherent with previous ones from Laurenz *et al.* (2016) and Steenstra *et al.* (2022) who did not explicitly propose an effect of silicate composition. Nevertheless, it is not possible to directly compare our coefficients with theirs, since the regression used is not the same.

Other models that include compositional effects previously predicted stronger effects of pressure (−190 and −265.8 for Blanchard *et al.*, 2021 model 2 and Smythe *et al.*, 2017 respectively), and either a stronger temperature term (−14683 in Smythe *et al.*, 2017) or even positive ones (18159 in the model 2 from Blanchard *et al.*, 2021).

In Figure S-3, we compare the SCSS values measured in the experimental runs with those calculated from Equation 2. This figure highlights the excellent agreement between our model and experimental data, despite the wide P–T compositional range studied here.

We also tested the effect of including only high P–T data to derive the evolution of SCSS. This is discussed in the Supplementary Information.

Discussion

The solubility of sulfur at sulfide saturation (SCSS) predicted from this work (Eq. 2) can be used to better understand the behaviour of sulfur during Earth's formation and differentiation.

The behaviour of sulfur in the Earth's magma ocean is of great importance, because many elements are chalcophile (sulfur-loving), hence their fate during episodes of melting is directly linked to that of sulfur. We have calculated SCSS as a function of pressure and temperature in a different context. First, we present in Figure 2a and 2b the evolution of SCSS along an adiabatic temperature profile for a magma ocean with a basal pressure of 80 GPa and 20 GPa (Miller *et al.*, 1991) respectively. For models that have a composition dependency, we used the composition of the PUM (Primitive Upper Mantle) from Palme and O'Neill (2014). From this figure, we observe that models of SCSS built from relatively low P–T experiments have a much more dramatic evolution, with higher starting SCSS values evolving toward much lower ones at high pressure. This is especially true for the 80 GPa adiabat, where for instance the Laurenz *et al.* (2016) model starts at values way higher than 1.5 wt. % of sulfur of SCSS to finish at 35 ppm at 80 GPa. Conversely, models built with both low and high P–T experiments (this study; Steenstra *et al.*, 2022) show a decrease (especially for 80 GPa adiabat), but it is much less intense. In our case, we predict an evolution of SCSS from about 11750 ppm at 0 GPa to about 4060 ppm at 80 GPa adiabat. For the 20 GPa adiabat, our study predicts almost a flat evolution (from about 6400 to about 5200 ppm), coherent with predictions from Steenstra *et al.* (2022). Again, models obtained from large volume press experiments predict a much stronger decrease of SCSS with pressure (Laurenz *et al.*, 2016; Smythe *et al.*, 2017; Blanchard *et al.*, 2021), with almost an order of magnitude difference for Laurenz *et al.* (2016). All in all, we predict for both low and high pressure adiabat high values of SCSS (>2500 ppm), in contrast to previous models obtained at lower P–T conditions.

It has been suggested that at the end of accretion, an episode of Hadean Matte occurred, during which ponds of FeS segregated from the magma ocean, due to the saturation of the magma ocean in sulfur (O'Neill, 1991). Using our formalism, we can now assess whether the terrestrial magma ocean ever reached sulfur saturation over the course of its existence.

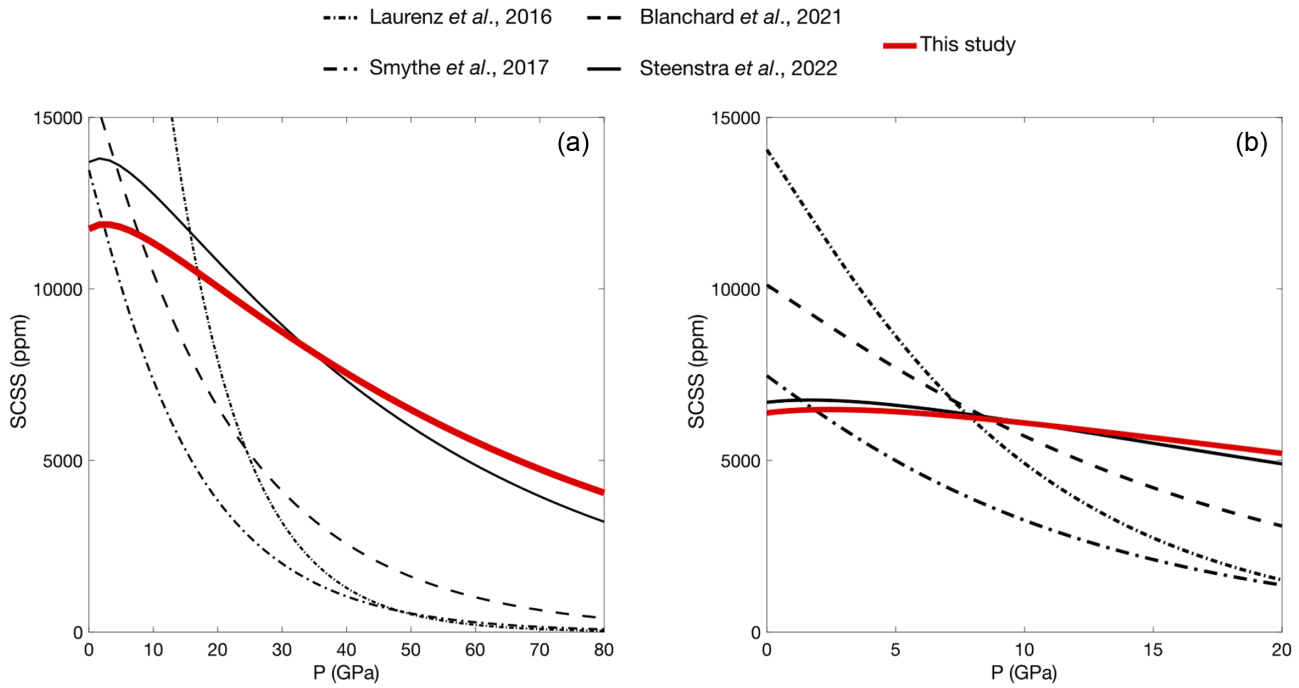

Figure 2 Evolution of SCSS as a function of pressure for 80 GPa adiabat **(a)** and 20 GPa adiabat **(b)**. For models that are composition dependent, we used Primitive Upper Mantle composition by (Palme and O'Neill, 2014).

The parameterisation derived in Equation 2 was used in a core formation model to assess the evolution of SCSS during the magma ocean phase on Earth. The temperature of the magma ocean was fixed as the arithmetic mean of the mantle liquidus proposed by Fiquet *et al.* (2010) and Andrault *et al.* (2011), and the depth of the magma ocean was fixed at 40 % of the mantle's depth at each stage. The core formation model was discretised into 100 steps, each representing the accretion of 1 % of Earth's mass. We have also tested the effect of changing fO_2 over the course of accretion by changing the amount of FeO, since the redox path of Earth's formation is a matter of debate (*e.g.*, Siebert *et al.*, 2013; Rubie *et al.*, 2016). Three different scenarios were tested: one where the fO_2 is increasing over the course of accretion from IW−4.5 to IW−2.3, one where fO_2 decreases from IW−1.3 to IW−2.3, and one constant fO_2 of IW−2.3. Figure 3 presents the evolution of SCSS with the accreted fraction of the Earth, following Equation 2, and changing fO_2 conditions as detailed previously. The composition of the silicate is fixed to the composition of the Primitive Upper Mantle proposed by Palme and O'Neill (2014) in the case of the constant fO_2, and the amount of FeO is varied for the two other redox paths. Given the importance of FeO in the evolution of SCSS (see Eq. 2), we additionally varied its abundance on the mantle on the two other redox paths through the course of accretion.

Rubie *et al.* (2016) were first to define empirically an effective pressure that describes SCSS and equilibration pressure for the entire magma ocean ($P_{eq-s} = k_S \times P_{CMB}$), provided that the corresponding temperature is between the liquidus and solidus of peridotite. It was shown by Steenstra *et al.* (2022) that k_S can range from 0.3 to 0.9 without impacting the evolution of SCSS, so we did not try to vary this value. Here, we used a constant value of 0.4, as suggested by Rubie *et al.* (2016). To assess whether the magma ocean ever reached SCSS, we compared the estimation of sulfur concentration at saturation with the residual amount of sulfur in the magma ocean due to metal-silicate partitioning during core formation. Figure 3 shows the amount of sulfur in the mantle predicted from metal-silicate partitioning experiments by Suer *et al.* (2017). We tested two homogeneous accretion scenarios: one where the magma ocean fully equilibrates with the forming core, and another where partial equilibration occurs between the magma ocean and the core (Deguen *et al.*, 2014). In this second scenario, equilibration is complete during the first 80 %, but becomes partial during the later stages of accretion when larger bodies are accreted (Suer *et al.*, 2017).

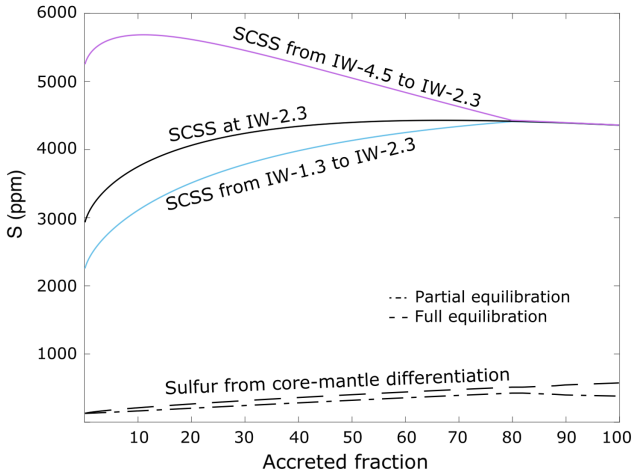

Figure 3 Comparison between the evolution of SCSS over the course of accretion from Equation 2, and the amount of sulfur in the magma ocean linked to core-mantle differentiation for both partial and full metal-silicate equilibration from Suer *et al.* (2017). The evolution of SCSS over the course of accretion is shown at constant fO_2 (black solid curve), in an oxidised scenario (purple curve), and in a reduced scenario (blue curve).

Regardless of the extent of equilibration, the model suggests that a maximum of about 500 ppm of sulfur can be stored in the magma ocean linked to core-mantle differentiation. This is far below the estimated SCSS, which is shown to be always higher than 2500 ppm, irrespective of the evolution of redox over the course of accretion (see Fig. 3). This is also true using a model derived only from high P–T experiments (see Supplementary Information, and Fig. S-4).

It has been proposed that oxygen can influence the partitioning of sulfur between metal and silicate (*e.g.*, Gendre *et al.*, 2022). We could not include the effect of oxygen on SCSS due to insufficient data. However, extrapolating data from Gendre *et al.* (2022) obtained at relatively low P–T conditions (<12 GPa and <2473 K) to core formation conditions would only strengthen our conclusions, as the presence of oxygen in the metallic phase enhances the siderophility of sulfur.

As can be seen in Figure 3, we predict a high SCSS during the whole course of accretion, with values above 2500 ppm, but a low concentration of sulfur predicted from metal-silicate partitioning experiments (<500 ppm). Previous experiments and models proposed by Steenstra *et al.*, (2022) are comparable to our results, although they predict slightly lower values of SCSS at the end of accretion (about 3500 ppm). In addition to a significant increase of the investigated pressure range, the main difference with our results is that we incorporate new high P–T data points with the effects of FeO and SiO_2 present in the silicate on SCSS. These results suggest that saturation of the magma ocean in sulfur was probably never reached over the course of accretion.

These estimations differ significantly from those of Rubie *et al.* (2016), who proposed up to about 7000 ppm of S in the mantle at the end of accretion. The difference stems from major differences in the accretion models. Rubie *et al.* (2016) considered that a large part of planetesimals that built the Earth were undifferentiated (fully oxidised). The evolution of SCSS they proposed is based on relatively low P–T experiments, that are very rich in HSEs (Laurenz *et al.*, 2016). Interactions of HSEs with sulfur are poorly constrained, but given that HSEs are chalcophile, their presence in the metallic phase of the runs could influence sulfur behaviour. Laurenz *et al.* (2016) propose a strong decrease of SCSS with increasing pressure, leading to sulfur saturation in a deep enough magma ocean. Consequently, Rubie *et al.* (2016) proposed that during the course of accretion, the magma ocean experienced at least one episode of sulfide liquid segregation, which stripped HSEs from Earth's mantle. They suggested that a subsequent episode of late accretion is mandatory to reproduce suprachondritic Pd/Ir and Ru/Ir ratios observed in today's mantle, and remove the excess of HSEs (Becker, 2006; Walker *et al.*, 2015). In light of our new high P–T experiments, we suggest that sulfide saturation was likely never reached during Earth's accretion (see Fig. 3). Hence, the proposition that HSE's mantle signatures can be explained by sulfide segregation early in the Earth's history appears unlikely.

Recent work have proposed that a significant decrease in the metal-silicate partitioning of platinum during core formation might explain abundance of this HSE in today's mantle (Suer *et al.*, 2021), rather than a combined effect of sulfide saturation and a late arrival of this element.

Acknowledgments

We would like to thank Edgar Steenstra, an anonymous reviewer and the editor of this paper, Ambre Luguet, for their constructive and helpful comments. We thank James Badro for laser heating the samples. The LHDAC lab is supported by the LabEx UnivEarthS, ANR-10-LABX-0023 and ANR-18-IDEX-0001. Parts of this work were supported by IPGP multidisciplinary programme PARI, and by Paris–IdF region SESAME Grant no. 12015908. We acknowledge Anja Schreiber from GFZ who extracted the FIB lamellae, Stephan Borensztajn from IPGP who helped us with SEM analyses. JS acknowledges support from the French National Research Agency (ANR project VolTerre, grant No. ANR-14-CE33-0017-01) and support from the Institut Universitaire de France.

Editor: Ambre Luguet

Additional Information

Supplementary Information accompanies this letter at https://www.geochemicalperspectivesletters.org/article2506.

Cite this letter as: Blanchard, I., Siebert, J., Kubik, E., Minchenkova, A., Calvo, L., Wehr, N. (2025) Earth's deep magma ocean never reached sulfide saturation. *Geochem. Persp. Let.* 34, 6–10. https://doi.org/10.7185/geochemlet.2506

References

Andrault, D., Bolfan-Casanova, N., Nigro, G.L., Bouhifd, M.A., Garbarino, G., Mezouar, M. (2011) Solidus and liquidus profiles of chondritic mantle: Implication for melting of the Earth across its history. *Earth Planetary Science Letters* 174, 181–191. https://doi.org/10.1016/j.epsl.2011.02.006

Becker, H., Horan, M.F., Walker, R.J., Gao, S., Lorand, J.-P., Rudnick, R.L. (2006) Highly siderophile element composition of the Earth's primitive upper mantle : Constraints from new data on peridotite massifs and xenoliths. *Geochimica Cosmochimica Acta* 70, 4528–4550. https://doi.org/10.1016/j.gca.2006.06.004

Blanchard, I., Siebert, J., Borensztajn, S., Badro, J. (2017) The solubility of heat-producing elements in Earth's core. *Geochemical Perspective Letters* 1–5. https://doi.org/10.7185/geochemlet.1737

Blanchard, I., Abeykoon, S., Frost, D.J., Rubie, D.C. (2021) Sulfur content at sulfide saturation of peridotitic melt at upper mantle conditions. *American Mineralogist* 106, 1835–1843. https://doi.org/10.2138/am-2021-7649

Blanchard, I., Rubie, D.C., Jennings, E.S., Franchi, I.A., Zhao, X., Petitgirard, S., Miyajima, N., Jacobson, S.A., Morbidelli, A. (2022) The metal–silicate partitioning of carbon during Earth's accretion and its distribution in the early solar system. *Earth Planetary Science Letters* 580, 117374. https://doi.org/10.1016/j.epsl.2022.117374

Deguen, R., Landeau, M., Olson, P. (2014) Turbulent metal–silicate mixing, fragmentation, and equilibration in magma oceans. *Earth Planetary Science Letters* 391, 274–287. https://doi.org/10.1016/j.epsl.2014.02.007

Fiquet, G., Auzende, A.L., Siebert, J., Corgne, A., Bureau, H., Ozawa, H., Garbarino, G. (2010) Melting of peridotite to 140 gigapascals. *Science* 329, 1516–1518. https://doi.org/10.1126/science.1192448

Fischer, R.A., Cottrell, E., Hauri, E., Lee, K.K.M., Le Voyer, M. (2020) The carbon content of Earth and its core. *Proceedings National Acadamey of Sciences U.S.A.* 117, 8743–8749. https://doi.org/10.1073/pnas.1919930117

Fortin, M., Riddle, J., Desjardins-langlais, Y., Baker, D.R. (2015) The effect of water on the sulfur concentration at sulfide saturation (SCSS) in natural melts. *Geochimica Cosmochimica Acta* 160, 100–116. https://doi.org/10.1016/j.gca.2015.03.022

Gendre, H., Badro, J., Wehr, N., Borensztajn, S. (2022) Martian core composition from experimental high-pressure metal-silicate phase equilibria. *Geochemical Perspective Letters* 21, 42–46. https://doi.org/10.7185/geochemlet.2216

Huang, D., Siebert, J., Badro, J. (2021) High pressure partitioning behavior of Mo and W and late sulfur delivery during Earth's core formation. *Geochimica Cosmochimica Acta* 310, 19–31. https://doi.org/10.1016/j.gca.2021.06.031

Laurenz, V., Rubie, D.C., Frost, D.J., Vogel, A.K. (2016) The importance of sulfur for the behavior of highly-siderophile elements during Earth's differentiation. *Geochimica Cosmochimica Acta* 194, 123–138. https://doi.org/10.1016/j.gca.2016.08.012

Li, J., Agee, C.B. (1996) Geochemistry of mantle-core differentiation at high pressure. *Nature* 381, 686–689. https://doi.org/10.1038/381686a0

Liu, Y., Samaha, N., Baker, D.R. (2007) Sulfur concentration at sulfide saturation (SCSS) in magmatic silicate melts. *Geochimica Cosmochimica Acta* 71, 1783–1799. https://doi.org/10.1016/j.gca.2007.01.004

Miller, G.H., Stolper, E.M., Ahrens, T.J. (1991) The equation of state of a molten komatiite 2. Application to komatiite petrogenesis and the Hadean mantle. *Journal of Geophysical Research* 96, 849–864. https://doi.org/10.1029/91jb01203

Namur, O., Charlier, B., Holtz, F., Cartier, C., McCammon, C. (2016) Sulfur solubility in reduced mafic silicate melts: Implications for the speciation and distribution of sulfur on Mercury. *Earth Planetary Science Letters* 448, 102–114. https://doi.org/10.1016/j.epsl.2016.05.024

O'Neill, H.S.C. (1991) The origin of the Moon and the early history of the Earth—A chemical model. Part 2: The Earth. *Geochimica Cosmochimica Acta* 55, 1159–1172. https://doi.org/10.1016/0016-7037(91)90169-6

O'Neill, H.S.C., Mavrogenes, J.A. (2002) The Sulfide Capacity and the Sulfur Content at Sulfide Saturation of Silicate Melts at 1400°C and 1 bar. *Journal of Petrology* 43, 1049–1087. https://doi.org/10.1093/petrology/43.6.1049

Palme, H., O'Neill, H.S.C. (2014) Cosmochemical Estimates of Mantle Composition, in: *Treatise on Geochemistry* 2nd Edition. Elsevier Ltd., pp. 1–39. https://doi.org/10.1016/B978-0-08-095975-7.00201-1

Rubie, D.C., Laurenz, V., Jacobson, S.A., Morbidelli, A., Palme, H., Vogel, A.K., Frost, D.J. (2016) Highly siderophile elements were stripped from Earth's mantle by iron sulfide segregation. *Science* 353, 1141–1144. https://doi.org/10.1126/science.aaf6919

Siebert, J., Badro, J., Antonangeli, D., Ryerson, F.J. (2012) Metal–silicate partitioning of Ni and Co in a deep magma ocean. *Earth Planetary Science Letters* 321–322, 189–197. https://doi.org/10.1016/j.epsl.2012.01.013

Siebert, J., Badro, J., Antonangeli, D., Ryerson, F.J. (2013) Terrestrial accretion under oxidizing conditions. *Science* 339, 1194–1197. https://doi.org/10.1126/science.1227923

Smythe, D.J., Wood, B.J., Kiseeva, E.S. (2017) The S content of silicate melts at sulfide saturation: New experiments and a model incorporating the effects of sulfide composition. *American Mineralogist* 102, 795–803. https://doi.org/10.2138/am-2017-5800CCBY

Steenstra, E.S., Lord, O.T., Vitale, S., Bullock, E.S., Klemme, S., Walter, M. (2022) Sulfur solubility in a deep magma ocean and implications for the deep sulfur cycle. *Geochemical Perspective Letters* 22, 5–9. https://doi.org/10.7185/geochemlet.2219

Suer, T.A., Siebert, J., Remusat, L., Menguy, N., Fiquet, G. (2017) A sulfur-poor terrestrial core inferred from metal–silicate partitioning experiments. *Earth Planetary Science Letters* 469, 84–97. https://doi.org/10.1016/j.epsl.2017.04.016

Suer, T.-A., Siebert, J., Remusat, L., Day, J.M.D., Borensztajn, S., Doisneau, B., Fiquet, G. (2021) Reconciling metal–silicate partitioning and late accretion in the Earth. *Nature Communications* 12. https://doi.org/10.1038/s41467-021-23137-5

Walker, R.J., Bermingham, K., Liu, J., Puchtel, I.S., Touboul, M., Worsham, E.A. (2015) In search of late-stage planetary building blocks. *Chemical Geology* 411, 125–142. https://doi.org/10.1016/j.chemgeo.2015.06.028

Wykes, J.L., O'Neill, H.S.C., Mavrogenes, J.A. (2015) The effect of FeO on the sulfur content at sulfide saturation (SCSS) and the selenium content at selenide saturation of silicate melts. *Journal of Petrology* 56, 1407–1424. https://doi.org/10.1093/petrology/egv041

ZhangZhou, J., Li, Y., Chowdhury, P., Sen, S., Ghosh, U., Xu, Z., Liu, J., Wang, Z., Day, J.M.D. (2024) Predicting sulfide precipitation in magma oceans on Earth, Mars and the Moon using machine learning. *Geochimica Cosmochimica Acta* 366, 237–249. https://doi.org/10.1016/j.gca.2023.11.029

Earth's deep magma ocean never reached sulfide saturation

I. Blanchard, J. Siebert, E. Kubik, A. Minchenkova, L. Calvo, N. Wehr

Supplementary Information

The Supplementary Information includes:

- Methods and Data Selection
- Tables S-1 and S-2
- Figures S-1 and S-2
- Supplementary Information References

Methods

The objective of this work is to determine the amounts of sulfur that can be stored in the magma ocean at sulfur saturation. To this end, we performed a series of laser heated diamond anvil cell experiments at the putative P–T conditions of Earth's differentiation. We synthetized five samples between 53 and 72 GPa and 3800 to 4050 K. Following previous studies, the starting materials consisted of either a pyrolytic or a basaltic glass, both synthetized by aerodynamic levitation, subsequently polished down to a thickness of 20 microns, then machined into discs of 80-120 microns in diameter using a femto-second laser at Institut de Physique du Globe de Paris (IPGP, Blanchard *et al.*, 2017, 2022) . The metallic component was pure FeS powder. We used 200- to 300-microns cullet diamonds. For each run, we first pre-indented a 250-microns thick rhenium gasket to a thickness of about 50 microns, then drilled an experimental chamber of about 120 microns in diameter. FeS powder was subsequently loaded in between two silicate discs before starting compression. We controlled the pressure by using the Raman shift of the diamond anvil (Akahama and Kawamura, 2004). Once we reached the targeted pressure, we heated our samples for 10 to 120 seconds in IPGP, using a double-sided laser heating system. Temperature conditions and chosen time durations were such that both the sulfur and the silicate were

molten and closely approached chemical equilibrium, given the small size of our runs. The reported pressure was corrected for thermal pressure following Siebert *et al*., (2012).

The experiments were terminated by switching off the laser power, which results in extremely fast quench due to the high thermal conductivity of the diamonds. Experiments were subsequently slowly decompressed to atmospheric pressure, and the region of interest was extracted using Ga-Focused Ion Beam (FIB) facility at the GeoForschung Zentrum (GFZ) in Potsdam, Germany. Chemical analysis of sulfides and quenched melt were performed at IPGP using Scanning electron microscopy energy dispersive X-rays (EDX), equipped with a Field Emission Gun. Standards of FeS_2 were used for sulfur, wollastonite for Ca and Si, and pure Al_2O_3, MgO and NaCl for Al, Mg and Na respectively. Results are presented in Table S-1.

Oxygen fugacity calculation

We calculated the oxygen fugacity of our experiments relative to the iron-wüstite buffer (ΔIW). We have expressed the ideal oxygen fugacity of each of our runs following:

$$\Delta IW = 2\log\frac{X_{FeO}}{X_{Fe}} \quad \text{Eq. (S1)}$$

With X_{FeO} and X_{Fe} the mole fractions of FeO in the silicate and of Fe in the metal respectively. The assumption of ideal mixing in both phases is justified by the high temperatures of our runs, as done in previous experiments (e.g., Blanchard *et al*., 2017; Fischer *et al*., 2020; Huang *et al*., 2021).

Data selection

We explicitly excluded data for which the starting sulfide was not pure FeS (i.e., data containing Cu, Ni for instance), those with silicate compositions far from a pyrolytic composition (i.e., containing significant wt. % of TiO_2, H_2O and/or Na_2O), and experiments performed using graphite capsule. Importantly, data obtained in extremely reduced system with very low FeO content (<0.5 wt. %) were also excluded. This is because the influence of FeO at those conditions is not linear, and tends to a U-shaped curve (O'Neill and Mavrogenes, 2002). We have plotted on figure S-1 all the literature data used in our regression used along with the new ones from this study. We can see a clear effect of pressure, temperature, SiO_2 and FeO on SCSS. From this

figure, we can also see that the pressure domain has been extended by 20 GPa compared to previous experimental data, reaching now 72 GPa.

Comparison with data from Steenstra et al., 2022

Here, we report experimental results on SCSS at wider P-T conditions than previous studies with MORB-like silicate composition (Steenstra *et al*., 2022). We also observe that for similar FeO concentrations on the run products, SCSS derived by Steenstra *et al*., (2022) is lower than in our pyrolytic composition. The reproducibility between our single experiment with MORB-like starting material (SCSS4), and those of Steenstra *et al*., (2022), suggests that compositional factor on the silicate phase plays a significant role on sulfur storage on silicate melts. As observed in Wykes *et al*., (2014) and reported in Steenstra *et al*., (2022), we observe a correlation between SCSS-FeO, and SCSS-SiO_2, where pyrolite hosts more sulfur upon saturation. Given that SCSS increases with increasing FeO and decreasing SiO_2, we consider of importance to model it as a function of the composition of the silicate melt, which has not been performed previously (Steenstra *et al*., 2022). Through this approach, a model for predicting SCSS in a more realistic early Earth composition can be achieved.

Model of SCSS using only high P-T data

There is no experimental data between 23 and 43 GPa, which is a region where structural changes can occur, especially due to the increase of silicon coordination (Sanloup *et al*., 2013). Hence, we have also modelled the dependency of SCSS on P, T, X_{SiO2} and X_{FeO} using only data obtained at the putative conditions of core formation (i.e. > 30 GPa and > 3000 K). The only data that exist on this range are the ones presented in this study, along with the ones of (Steenstra *et al*., 2022), which makes only eight experimental data. We regressed those data with Eq. 2 presented in main text. We obtained the following regression, with uncertainties in brackets:

$$\ln S_{SCSS} = 10\ (0.5) - \frac{2959\ (2207)}{T} + 3.7(16)\frac{P}{T} + \frac{76\ 212\ (2861)}{T} \times X_{FeO} - \frac{25\ 333\ (4047)}{T} \times X_{SiO2} \quad \text{Eq. (S2)}$$

As can be seen, the pressure term is not relevant, so we did a second round of regression, excluding the pressure effect. By doing so, we obtain:

$$\ln S_{SCSS} = 10\ (0.5) - \frac{3327\ (1503)}{T} + \frac{7135\ (1908)}{T} \times X_{FeO} - \frac{25\ 695\ (3732)}{T} \times X_{SiO2} \quad \text{Eq. (S3)}$$

In this last regression (Eq. S3), the terms are evidently different from Eq. 2 (main text), but they display the same sign, and have smaller uncertainties.

Subsequently, we have included this regression in a model of magma ocean, as we presented in the main text. As can be seen in Fig. S-4, the evolution of SCSS over the course of accretion is different from the one presented in the main text and in Fig. 3, but the message holds. Indeed, regardless of the redox path, we still see that SCSS is way higher than the amount of sulfur present in the mantle due to core-mantle differentiation.

Supplementary Tables

Table S-1 Compositions of the experimental run products

Run #	SCSS1		SCSS2		SCSS3		SCSS4		SCSS5	
Silicate wt. %	N=8		N=13		N=9		N=16		N=13	
MgO	36.38	0.32	36.00	0.53	39.83	0.2	10.35	0.13	36.17	0.42
Al_2O_3	6.69	0.15	5.92	0.22	5.99	0.11	21.45	0.42	5.71	0.26
SiO_2	37.53	0.86	37.65	0.89	39.18	0.30	39.66	1.89	40.27	0.67
CaO	4.24	0.10	3.97	0.10	3.87	0.08	5.64	0.30	4.30	0.08
FeO	14.14	0.88	15.33	1.15	9.98	0.40	19.29	1.34	12.63	1.01
Na_2O	-	-	-	-	-	-	2.79	0.05	-	-
S	1.02	0.27	1.12	0.36	1.15	0.15	0.83	0.31	0.93	0.25
Total	100		100		100		100		100	
sulfide wt. %	N=6		N=5		N=4		N=7		N=7	
O	6.92	0.27	7.17	0.78	5.80	0.80	9.76	0.41	5.82	0.64
Mg	0.80	0.19	0.74	0.15	1.04	0.32	0.18	0.10	0.66	0.15
Al	0.21	0.02	0.23	0.02	0.27	0.07	0.34	0.09	0.18	0.07
Si	0.64	0.13	0.69	0.10	1.17	0.21	1.06	0.12	0.58	0.16
S	28.27	0.42	25.51	0.39	28.15	0.57	26.86	0.36	28.80	0.70
Fe	63.17	0.28	65.66	0.70	63.57	0.85	61.80	0.40	63.96	0.47
Total	100		100		100		100		100	

Table S-2 Compilation of experimental runs used in this study**,** is available for download (.xlsx) from the online version of this article.

Supplementary Figures

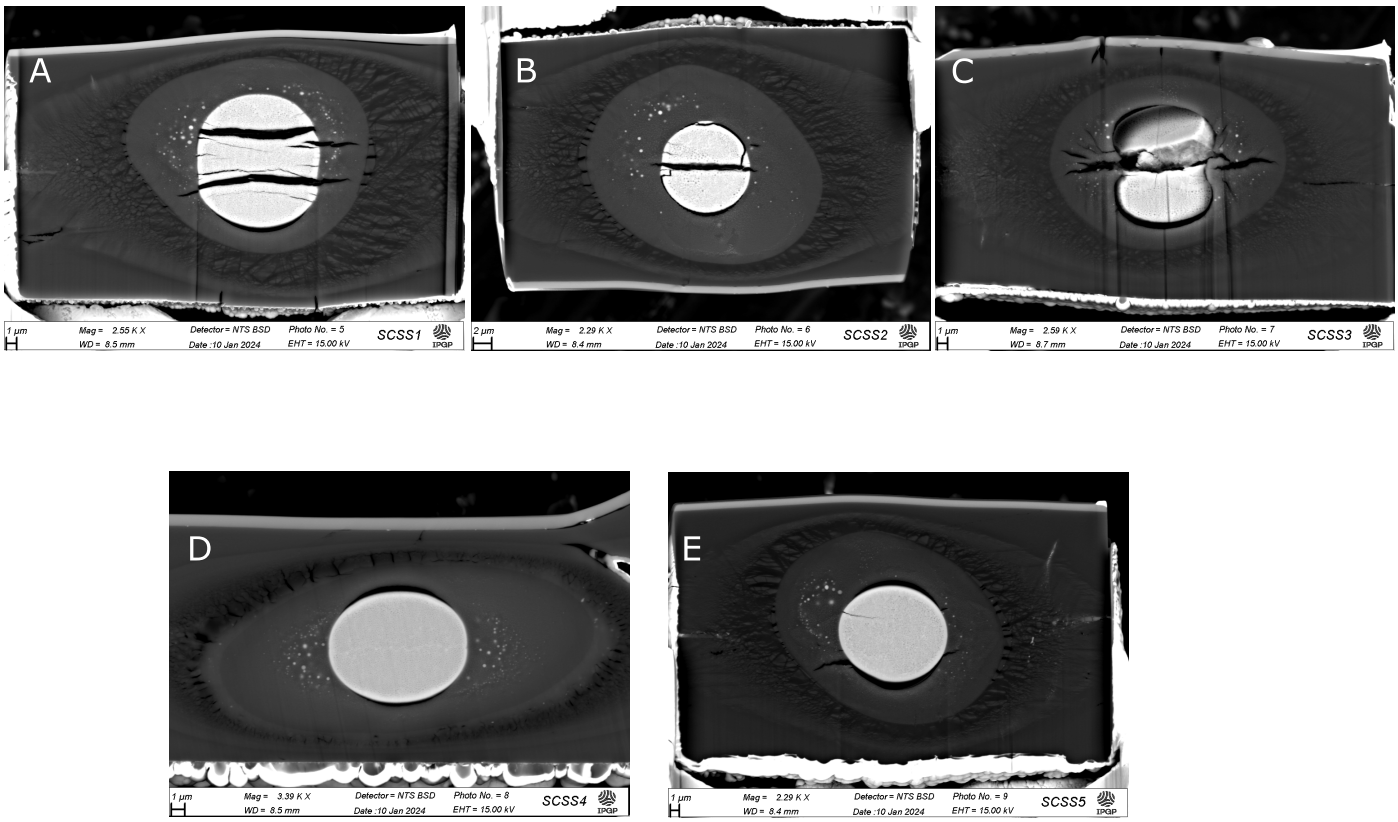

Figure S-1 Backscattered images of all our samples. A) SCSS1 synthesised at 64 GPa, 4000 K, B) SCSS2 synthesised at 61 GPa, 4000 K, C) SCSS3 synthesised at 72 GPa, 4050 K, D) SCSS4 synthesised at 53 GPa, 3800 K and E) SCSS5 synthesised at 53 GPa and 3800 K.

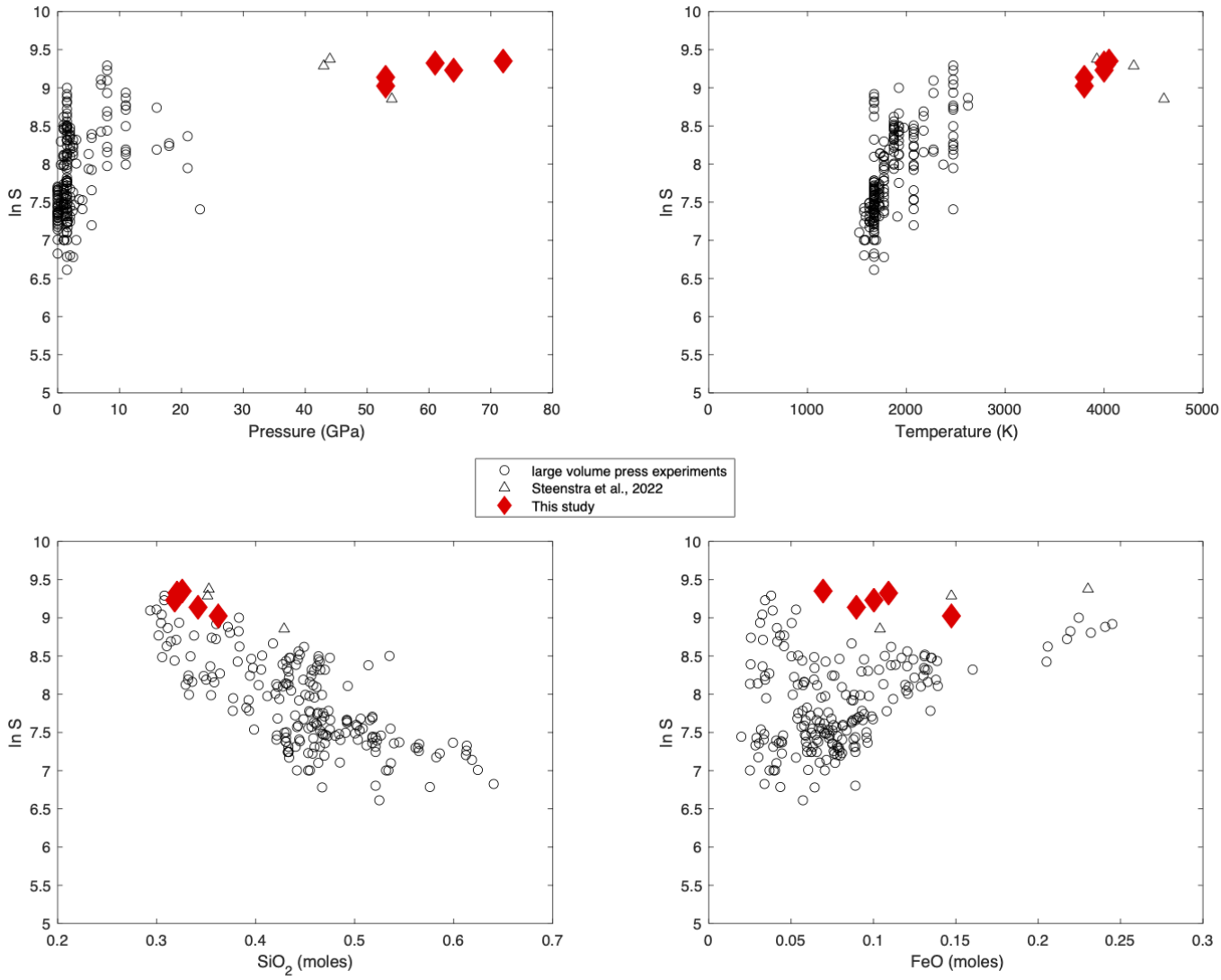

Figure S-2 Evolution of SCSS as a function of pressure, temperature, SiO_2 and FeO. Data labelled as large volume press experiments are from Wendlandt (1982); Mavrogenes and O'Neill (1999); O'Neill and Mavrogenes (2002); Holzheid and Grove (2002); Jugo *et al*., (2005); Liu *et al*., (2007); Kiseeva and Wood (2013); Ding *et al*., (2014); Wohlers and Wood (2015); Wood and Kiseeva (2015); Laurenz *et al*., (2016); Smythe *et al*., (2017); Blanchard *et al*., (2021).

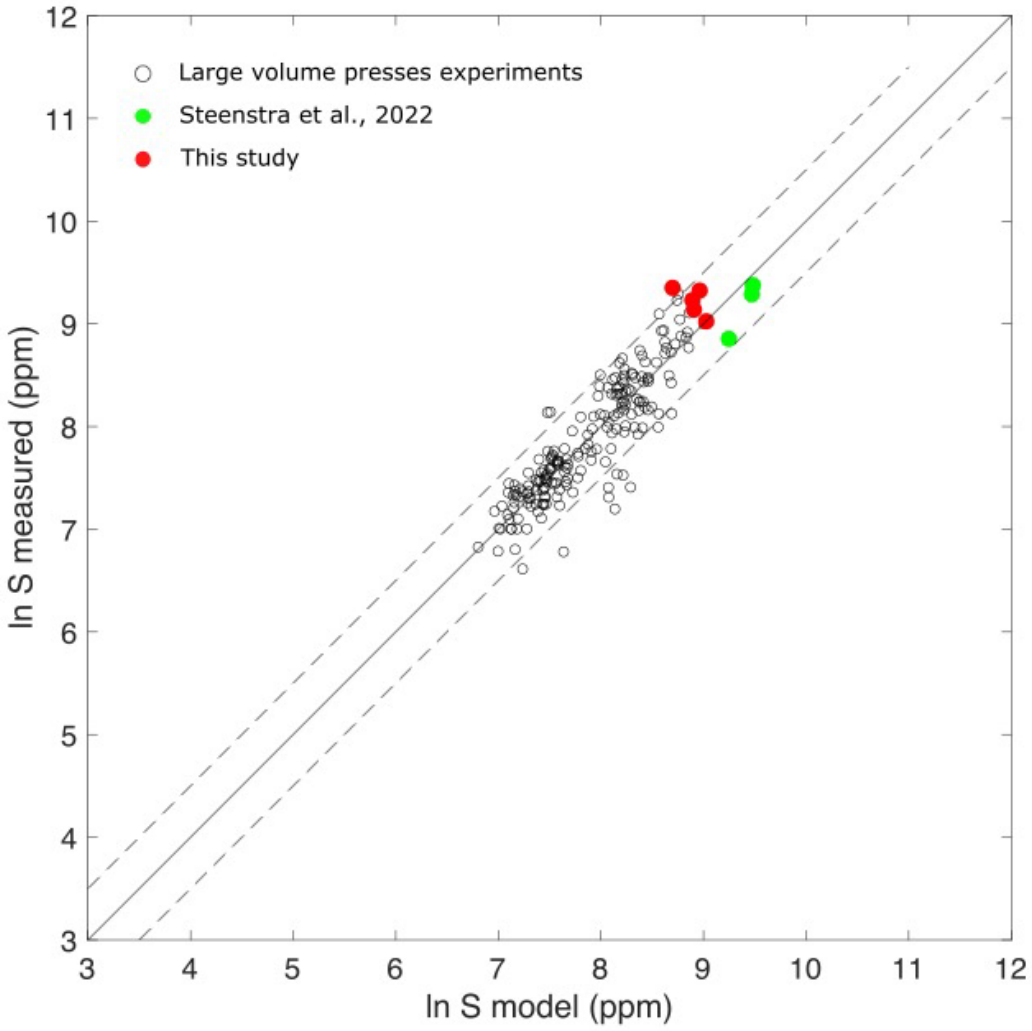

Figure S-3 Comparison between experimental data and results from our model (Eq. 2). Data from large volume presses experiments are from Wendlandt (1982); Mavrogenes and O'Neill (1999); O'Neill and Mavrogenes (2002); Holzheid and Grove (2002); Jugo *et al*., (2005); Liu *et al*., (2007); Kiseeva and Wood (2013); Ding *et al*., (2014); Wohlers and Wood (2015); Wood and Kiseeva (2015); Laurenz *et al*., (2016); Smythe *et al*., (2017); Blanchard *et al*., (2021).

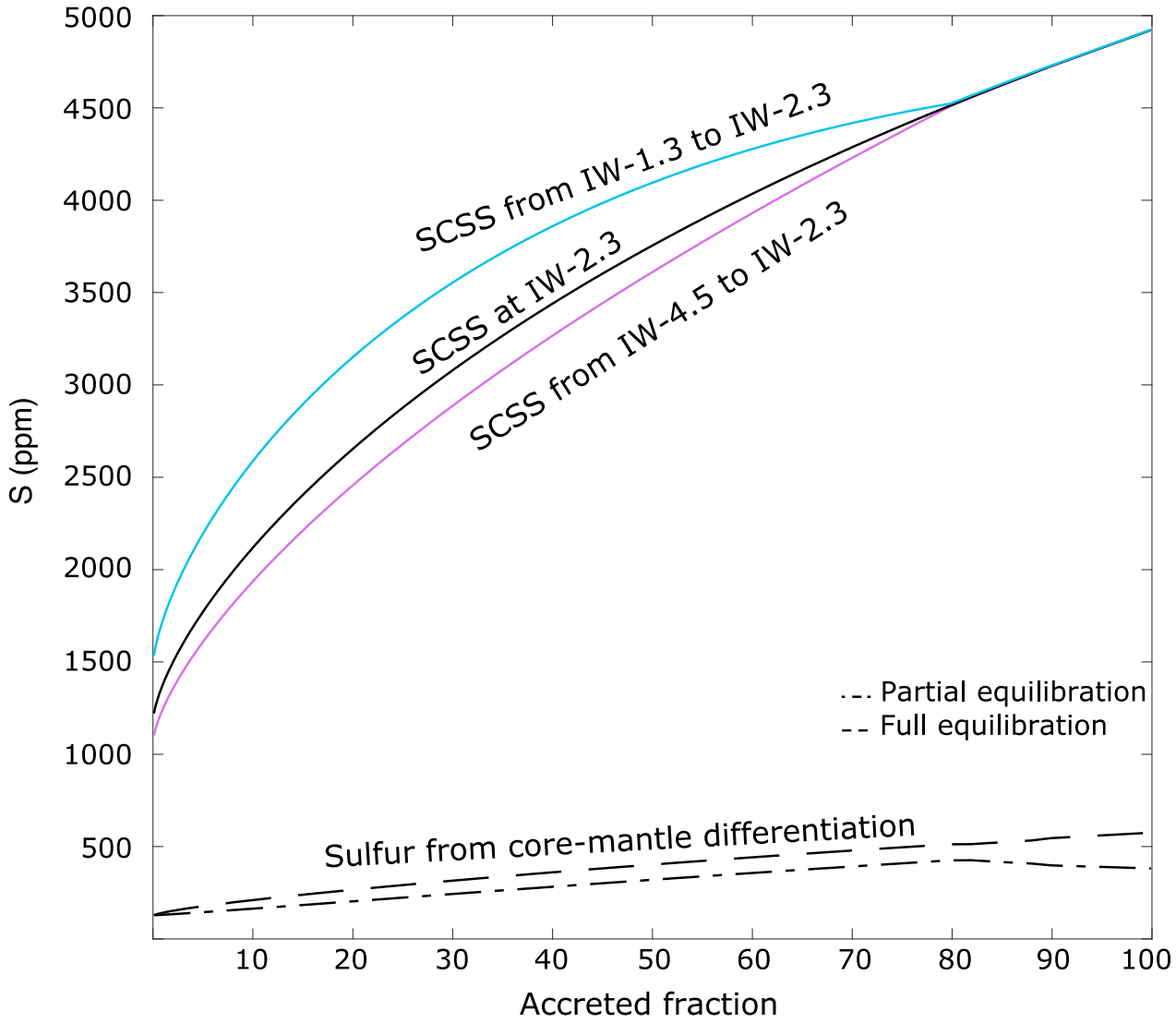

Figure S-4 Evolution of SCSS determined from Eq. S3, using only data obtained by diamond anvil-cell coupled with laser heating system (this study, Steenstra *et al*., 2022). Sulfur from core-mantle differentiation is calculated using Suer *et al*., (2017) model.

Supplementary Information References

Akahama, Y., Kawamura, H. (2004) High-pressure Raman spectroscopy of diamond anvils to 250 GPa: Method for pressure determination in the multimegabar pressure range. *Journal of Applied Physics* 96, 3748–3751.

Blanchard, I., Siebert, J., Borensztajn, S., Badro, J. (2017) The solubility of heat-producing elements in Earth's core. *Geochemical Perspectives Letters 5*, 1–5. https://doi.org/10.7185/geochemlet.1737

Blanchard, I., Abeykoon, S., Frost, D.J., Rubie, D.C. (2021) Sulfur content at sulfide saturation of peridotitic melt at upper mantle conditions. *American Mineralogist* 106, 1835–1843. https://doi.org/10.2138/am-2021-7649

Blanchard, I., Rubie, D.C., Jennings, E.S., Franchi, I.A., Zhao, X., Petitgirard, S., Miyajima, N., Jacobson, S.A., Morbidelli, A. (2022) The metal–silicate partitioning of carbon during Earth's accretion and its distribution in the early solar system. *Earth and Planetary Science Letters* 580, 117374. https://doi.org/10.1016/j.epsl.2022.117374

Ding, S., Dasgupta, R., Tsuno, K. (2014) Sulfur concentration of martian basalts at sulfide saturation at high pressures and temperatures - Implications for deep sulfur cycle on Mars. *Geochimica Cosmochimica Acta* 131, 227–246. https://doi.org/10.1016/j.gca.2014.02.003

Fischer, R.A., Cottrell, E., Hauri, E., Lee, K.K.M., Le Voyer, M. (2020) The carbon content of Earth and its core. *Proceedings of the National Academy of Sciences* 117, 8743–8749. https://doi.org/10.1073/pnas.1919930117

Holzheid, A., Grove, T.L. (2002) Sulfur saturation limits in silicate melts and their implications for core formation scenarios for terrestrial planets. *American Mineralogist* 87, 227–237. https://doi.org/10.2138/am-2002-2-304

Huang, D., Siebert, J., Badro, J. (2021) High pressure partitioning behavior of Mo and W and late sulfur delivery during Earth's core formation. *Geochimica Cosmochimica Acta* 310, 19–31. https://doi.org/10.1016/j.gca.2021.06.031

Jugo, P.J., Luth, R.W., Richards, J.P. (2005) An Experimental Study of the Sulfur Content in Basaltic Melts Saturated with Immiscible Sulfide or Sulfate Liquids at 1300 C and 1 GPa. *Journal of Petrology* 46, 783–798. https://doi.org/10.1093/petrology/egh097

Kiseeva, E.S., Wood, B.J. (2013) A simple model for chalcophile element partitioning between sulphide and silicate liquids with geochemical applications. *Earth and Planetary Science Letters* 383, 68–81. https://doi.org/10.1016/j.epsl.2013.09.034

Laurenz, V., Rubie, D.C., Frost, D.J., Vogel, A.K. (2016) The importance of sulfur for the behavior of highly-siderophile elements during Earth's differentiation. *Geochimica Cosmochimica Acta* 194, 123–138. https://doi.org/10.1016/j.gca.2016.08.012

Liu, Y., Samaha, N., Baker, D.R. (2007) Sulfur concentration at sulfide saturation (SCSS) in magmatic silicate melts. *Geochimica Cosmochimica Acta* 71, 1783–1799. https://doi.org/10.1016/j.gca.2007.01.004

Mavrogenes, J.A., O'Neill, H.S.C. (1999) The relative effects of pressure, temperature and oxygen fugacity on the solubility of sulfide in mafic magmas. *Geochimica Cosmochimica Acta* 63, 1173–1180. https://doi.org/10.1016/S0016-7037(98)00289-0

O'Neill, H.S.C., Mavrogenes, J.A. (2002) The Sulfide Capacity and the Sulfur Content at Sulfide Saturation of Silicate Melts at 1400°C and 1 bar. *Journal of Petrology* 43, 1049–1087. https://doi.org/10.1093/petrology/43.6.1049

Sanloup, C., Drewitt, J.W.E., Konôpková, Z., Dalladay-Simpson, P., Morton, D.M., Rai, N., Van Westrenen, W., Morgenroth, W. (2013) Structural change in molten basalt at deep mantle conditions. *Nature* 503, 104–107. https://doi.org/10.1038/nature12668

Siebert, J., Badro, J., Antonangeli, D., Ryerson, F.J. (2012) Metal–silicate partitioning of Ni and Co in a deep magma ocean. *Earth and Planetary Science Letters* 321–322, 189–197. https://doi.org/10.1016/j.epsl.2012.01.013

Smythe, D.J., Wood, B.J., Kiseeva, E.S. (2017) The S content of silicate melts at sulfide saturation: New experiments and a model incorporating the effects of sulfide composition. *American Mineralogist* 102, 795–803. https://doi.org/10.2138/am-2017-5800CCBY

Steenstra, E.S., Lord, O.T., Vitale, S., Bullock, E.S., Klemme, S., Walter, M. (2022) Sulfur solubility in a deep magma ocean and implications for the deep sulfur cycle. *Geochemical Perspectives Letters* 22, 5–9. https://doi.org/10.7185/geochemlet.2219

Suer, T.A., Siebert, J., Remusat, L., Menguy, N., Fiquet, G. (2017) A sulfur-poor terrestrial core inferred from metal–silicate partitioning experiments. *Earth and Planetary Science Letters* 469, 84–97. https://doi.org/10.1016/j.epsl.2017.04.016

Wendlandt, R.F. (1982) Sulfide saturation of basalt and andesite melts at high pressures and temperatures. *American Mineralogist* 67, 877–885.

Wohlers, A., Wood, B.J. (2015) A Mercury-like component of early Earth yields uranium in the core and high mantle ^{142}Nd. *Nature* 520, 337–340. https://doi.org/10.1038/nature14350

Wood, B.J., Kiseeva, E.S. (2015) Trace element partitioning into sulfide: How lithophile elements become chalcophile and vice versa. *American Mineralogist* 100, 2371–2379. https://doi.org/10.2138/am-2015-5358ccbyncnd

Wykes, J.L., O'Neill, H.S.C., Mavrogenes, J.A. (2014) The effect of FeO on the sulfur content at sulfide saturation (SCSS) and the selenium content at selenide saturation of silicate melts. *Journal of Petrology* 56, 1407–1424. https://doi.org/10.1093/petrology/egv041